

Measurement of incorporation kinetics of non-fluorescent native nucleotides by DNA polymerases using fluorescence microscopy

Matthew T. Walsh and Xiaohua Huang*

Department of Bioengineering, University of California, San Diego, 9500 Gilman Drive, La Jolla, CA 92093-0412, USA

Received April 26, 2017; Revised August 07, 2017; Editorial Decision September 09, 2017; Accepted September 11, 2017

ABSTRACT

We describe a method for measuring the single-turnover incorporation kinetics of non-fluorescent native nucleotides by DNA polymerases. Time-lapse total internal reflection fluorescence (TIRF) microscopy is used to directly measure the kinetics of single-base nucleotide incorporation into primed DNA templates covalently attached to the surface of a glass coverslip using a fixed ratio of a native nucleotide and a corresponding fluorescently labeled nucleotide over a series of total nucleotide concentrations. The presence of a labeled nucleotide allows for the kinetics of competitive incorporation reactions by DNA polymerase to be monitored. The single-turnover catalytic rate constants and Michaelis constants of the incorporation of the native nucleotides can be determined by modeling the kinetics of the parallel competitive reactions. Our method enables the measurements of the kinetics parameters of incorporation of native or other non-fluorescent nucleotides without using a rapid stopped-flow or quench-flow instrument and the generally more involved and less quantitative post-reaction analysis of the reaction products. As a demonstration of our method, we systematically determined the single-turnover incorporation kinetics of all four native nucleotides and a set of Cy3-labeled nucleotides by the Klenow fragment of *Escherichia coli* DNA polymerase I.

INTRODUCTION

DNA polymerases exhibit remarkably high fidelity in DNA replication. This great specificity for recognizing and catalyzing the incorporation of the correct incoming nucleotide, complementary to the base on the template, is due to the exquisite control over each stage in the multi-step chemo-mechanical process by the polymerases (1–4). This

stringent discrimination by DNA polymerases extends to chemically modified nucleotides as well (5). As a consequence, the efficient incorporation of modified nucleotides usually requires DNA polymerases that have been highly engineered to be capable of using modified nucleotides as the substrates. Chemically modified nucleotides have been essential in genomic research and other molecular biology techniques, such as next-generation DNA sequencing and microarray assays. Target detection by hybridization using DNA microarrays requires the labeling of nucleic acids with reactive groups or fluorescent dyes during transcription or DNA replication process (6). For the microarray studies, the ratio of the chemically-labeled nucleotides to native nucleotides must be carefully tuned to obtain the proper degree of labeling to produce full length product with minimal dye quenching and hindrance to hybridization (7). The current generation of high throughput sequencing technologies also relies on the use of nucleotides labeled with fluorophores and the incorporation of the labeled nucleotides by engineered DNA polymerases (8–10). In these applications, it is useful and sometimes essential to know the kinetics of nucleotide incorporation by either natural or engineered DNA polymerases, and the bias of the polymerases toward native nucleotides over modified nucleotides (11). Quantitative characterization of incorporation kinetics by DNA polymerases, however, is not trivial, requiring substantial efforts and specialized instruments. Most traditional methods for measuring DNA polymerase kinetics rely on chemical quench-flow or stopped-flow methods followed by various analyses using electrophoretic separation or binding and quantification of radioactively labeled products. Other reported methods aim to simplify the analysis by combining stopped-flow with fluorescence measurement or using DNA polymerases or DNA substrates that are labeled with fluorescent probes sensitive to the local protein environment or conformations (12–15). Recently we have developed a method for the rapid and automated measurements of incorporation kinetics of fluorescently labeled nucleotides by DNA polymerases using an integrated system with microfluidics and TIRF microscopy (16).

*To whom correspondence should be addressed. Tel: +1 858 822 2155; Email: x2huang@ucsd.edu

In this work, we extend our method to enable the determination of incorporation kinetics of native nucleotides, as well as non-fluorescent modified nucleotides, which cannot be otherwise monitored directly using fluorescence microscopy. Standard methods for quantifying nucleotide incorporation kinetics are tedious. Our method significantly simplifies the process, enabling the rapid measurements of kinetic parameters. Our strategy is to first characterize the incorporation kinetics of a pure fluorescently labeled nucleotide at a series of nucleotide concentrations. Parallel competitive reactions between the incorporation of native and labeled nucleotides are then performed with a constant ratio of the labeled and native nucleotides, over a series of total nucleotide concentrations. By modeling the competitive reactions and quantifying the change in the incorporation kinetics of the pure fluorescently labeled nucleotide, the incorporation kinetics of the native nucleotides can be determined. The incorporation reactions by the DNA polymerase are performed on primed DNA templates anchored on a solid surface and the reactions are monitored directly in real time using TIRF microscopy, eliminating the need for post-reaction analysis of the products. Using a set of native and Cy3-labeled nucleotides, and the Klenow fragment of *Escherichia coli* DNA polymerase I, a well-characterized polymerase, we demonstrated that both the catalytic rate constants (k_2) and Michaelis constants or equilibrium nucleotide binding dissociation constant (K_M or K_d) of both native and labeled nucleotides can be determined.

MATERIALS AND METHODS

Materials

All chemicals are of ACS reagent grade unless specified otherwise. Synthetic oligonucleotides (oligos) were purchased from Integrated DNA Technologies. *Bst* DNA polymerase large fragment, terminal deoxyribonucleotidyl transferase (TdT), Klenow Fragment (3' → 5' exo-), and large fragment of *E. coli* DNA polymerase I (Klenow fragment) were purchased from New England BioLabs. Deionized water refers to MilliQ-purified 18 MΩ·cm water. Deoxyribonucleoside triphosphates (dNTPs) and a set dNTPs labeled with Cy3 dye were purchased from Jena Biosciences and stored in aliquots at -30°C. The concentrations of the stock solutions were measured using a spectrophotometer (PerkinElmer Lambda-20). The structures of the labeled nucleotides are shown in Supplementary Figure S1 in the Supplementary Materials. Protocatechuic acid (PCA), 6-hydroxy-2,5,7,8-tetramethylchroman-2-carboxylic acid (Trolox) and rotocatechuate-3,4-dioxygenase (PCD) used as oxygen-scavenging reagents were purchased from Sigma-Aldrich. Aminosilane coated coverglass (NEXTERION A+) was purchased from SCHOTT. Homo-bifunctional carboxymethyl polyethylene glycol with molecular weight of 1000 g/mol (dicarboxyl-PEG1000) was purchased from Laysan Bio, Inc.

Modeling parallel competitive incorporation of native and labeled nucleotides by DNA polymerases

In a previous report, we demonstrated a method for determining the kinetic parameters (k_2 and K_d) of the incor-

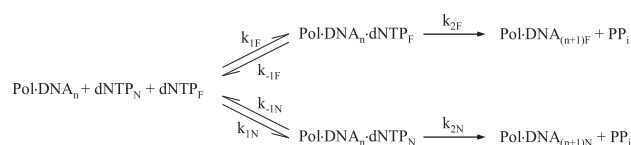


Figure 1. Parallel competitive reactions between the incorporation of a native nucleotide and a labeled nucleotide by a DNA polymerase. The subscript N is used to represent the native nucleotide (dNTP_N) and its extended product. The subscript F is used to represent the labeled nucleotide (dNTP_F) and its extended product. Pol·DNA_n represents the complex of polymerase and primer–DNA template with the last base of the primer hybridized to base n on the template strand. Pol·DNA_n·dNTP_N and Pol·DNA_n·dNTP_F represent the Pol·DNA_n complexes with a native nucleotide (dNTP_N) and labeled nucleotide (dNTP_F) bound at the active site of the polymerase, respectively. Pol·DNA_{(n+1)N} and Pol·DNA_{(n+1)F} are the one-base extension products with a native nucleoside and a labeled nucleoside incorporated into the primer, respectively. PP_i is the released inorganic pyrophosphate.

poration of pure labeled nucleotides by DNA polymerases (16). In this work, we have extended the method to the measurements of the incorporation kinetics of native nucleotides. Our strategy is to set up parallel competitive reactions for the incorporation of a labeled nucleotide and its corresponding native nucleotide. The use of the labeled nucleotides allows for the reactions to be followed using fluorescence microscopy. The parallel competitive reactions are illustrated in Figure 1.

To simplify the experimental measurements and the derivation of the integrated rate expressions for the kinetics, a large excess of nucleotides to the initial polymerase–primer/template complex is used to ensure that the nucleotide concentrations remain essentially constant. Since the rates of nucleotide binding to the polymerase–primer/template complex and the dissociation of nucleotide from the complex are known to be much faster than that of nucleotide incorporation ($k_1 \gg k_2$ and $k_{-1} \gg k_2$) (2), a rapid equilibrium is assumed to establish between the binding and dissociation of nucleotides, enabling the steady-state approximation to be applied to the intermediate complexes and allowing the reactions to be treated as two competing pseudo first-order reactions. To determine the kinetics parameters, the reactions are carried out with DNA polymerases bound to primer/templates tethered to a glass surface and TIRF microscopy is used to measure the accumulation of the extension product with the labeled nucleoside incorporated as a function of time, $d[\text{Pol} \cdot \text{DNA}_{(n+1)F}]/dt$. A brief derivation of the relationship is given below. More detail is given in the Supplementary Materials.

The application of the steady-state approximation to the intermediate complexes results in:

$$[\text{Pol} \cdot \text{DNA}_n \cdot \text{dNTP}_F] = \frac{K_{MF}^{-1} [\text{dNTP}_F] [\text{Pol} \cdot \text{DNA}_n]}{K_{MF} = (k_{-1F} + k_{2F})/k_{1F}} \quad (1)$$

$$[\text{Pol} \cdot \text{DNA}_n \cdot \text{dNTP}_N] = \frac{K_{MN}^{-1} [\text{dNTP}_N] [\text{Pol} \cdot \text{DNA}_n]}{K_{MN} = (k_{-1N} + k_{2N})/k_{1N}} \quad (2)$$

Using Equations (1) and (2), the rates of formation of the single-base extension products can be expressed as:

$$\frac{d[\text{Pol} \cdot \text{DNA}_{(n+1)\text{F}}]/dt}{k_{2\text{F}}[\text{Pol} \cdot \text{DNA}_n \cdot \text{dNTP}_{\text{F}}]} = k_{2\text{F}}K_{\text{MF}}^{-1}[\text{dNTP}_{\text{F}}][\text{Pol} \cdot \text{DNA}_n] \quad (3)$$

$$\frac{d[\text{Pol} \cdot \text{DNA}_{(n+1)\text{N}}]/dt}{k_{2\text{N}}[\text{Pol} \cdot \text{DNA}_n \cdot \text{dNTP}_{\text{N}}]} = k_{2\text{N}}K_{\text{MN}}^{-1}[\text{dNTP}_{\text{N}}][\text{Pol} \cdot \text{DNA}_n] \quad (4)$$

By dividing Equation (4) by Equation (3) and integrating the resultant equation, the concentration of $[\text{Pol} \cdot \text{DNA}_{(n+1)\text{N}}]$ can be related to $[\text{Pol} \cdot \text{DNA}_{(n+1)\text{F}}]$ as:

$$\frac{[\text{Pol} \cdot \text{DNA}_{(n+1)\text{N}}]}{(k_{2\text{N}}K_{\text{MN}}^{-1}[\text{dNTP}_{\text{N}}]/k_{2\text{F}}K_{\text{MF}}^{-1}[\text{dNTP}_{\text{F}}])[\text{Pol} \cdot \text{DNA}_{(n+1)\text{F}}]} = \quad (5)$$

By balancing the total concentration of all polymerase complexes and using Equations (1), (2) and (4), the concentration of $[\text{Pol} \cdot \text{DNA}_n]$ can be obtained:

$$[\text{Pol} \cdot \text{DNA}_n] = (1 + K_{\text{MF}}^{-1}[\text{dNTP}_{\text{F}}] + K_{\text{MN}}^{-1}[\text{dNTP}_{\text{N}}])^{-1} \left([\text{Pol} \cdot \text{DNA}_{\text{Total}}] - \left(1 + \frac{k_{2\text{N}}K_{\text{MN}}^{-1}[\text{dNTP}_{\text{N}}]}{k_{2\text{F}}K_{\text{MF}}^{-1}[\text{dNTP}_{\text{F}}]} \right) [\text{Pol} \cdot \text{DNA}_{(n+1)\text{F}}] \right) \quad (6)$$

The concentration of $[\text{Pol} \cdot \text{DNA}_{(n+1)\text{F}}]$ as a function of time can be solved for by substituting Equation (6) into Equation (3), and integrating the resultant equation:

$$[\text{Pol} \cdot \text{DNA}_{(n+1)\text{F}}] = a(1 - e^{-bt}), \quad (7)$$

where $a = \frac{k_{2\text{F}}K_{\text{MF}}^{-1}[\text{dNTP}_{\text{F}}]}{k_{2\text{F}}K_{\text{MF}}^{-1}[\text{dNTP}_{\text{F}}] + k_{2\text{N}}K_{\text{MN}}^{-1}[\text{dNTP}_{\text{N}}]} [\text{Pol} \cdot \text{DNA}_{\text{Total}}]$, $b = \frac{k_{2\text{F}}K_{\text{MF}}^{-1}[\text{dNTP}_{\text{F}}] + k_{2\text{N}}K_{\text{MN}}^{-1}[\text{dNTP}_{\text{N}}]}{1 + K_{\text{MF}}^{-1}[\text{dNTP}_{\text{F}}] + K_{\text{MN}}^{-1}[\text{dNTP}_{\text{N}}]}$.

If the ratio of labeled nucleotide to native nucleotide is r ($r = [\text{dNTP}_{\text{F}}]/[\text{dNTP}_{\text{N}}]$) and the total nucleotide concentration of the nucleotides is $[\text{dNTP}_{\text{Total}}]$ ($[\text{dNTP}_{\text{Total}}] = [\text{dNTP}_{\text{F}}] + [\text{dNTP}_{\text{N}}]$), the concentration of the labeled and native nucleotides can be expressed as $[\text{dNTP}_{\text{F}}] = r(1+r)^{-1}[\text{dNTP}_{\text{Total}}]$ and $[\text{dNTP}_{\text{N}}] = (1+r)^{-1}[\text{dNTP}_{\text{Total}}]$, and Equation (7) can be expressed as:

$$[\text{Pol} \cdot \text{DNA}_{(n+1)\text{F}}] = a(1 - e^{-bt}), \quad (8)$$

where $a = \frac{k_{2\text{F}}K_{\text{MF}}^{-1}r[\text{dNTP}_{\text{Total}}]}{k_{2\text{F}}K_{\text{MF}}^{-1}r[\text{dNTP}_{\text{Total}}] + k_{2\text{N}}K_{\text{MN}}^{-1}[\text{dNTP}_{\text{Total}}]} [\text{Pol} \cdot \text{DNA}_{\text{Total}}]$, $b = \frac{(k_{2\text{F}}K_{\text{MF}}^{-1}r + k_{2\text{N}}K_{\text{MN}}^{-1})(K_{\text{MF}}^{-1}r + K_{\text{MN}}^{-1})^{-1}[\text{dNTP}_{\text{Total}}]}{(K_{\text{MF}}^{-1}r + K_{\text{MN}}^{-1})^{-1}(1+r) + [\text{dNTP}_{\text{Total}}]}$.

When pure labeled nucleotide is used ($r = \infty$), Equation (8) is reduced to:

$$[\text{Pol} \cdot \text{DNA}_{(n+1)\text{F}}] = a(1 - e^{-bt}), \text{ where } a = [\text{Pol} \cdot \text{DNA}_{\text{Total}}], b = \frac{k_{2\text{F}}[\text{dNTP}_{\text{F}}]}{K_{\text{MF}} + [\text{dNTP}_{\text{F}}]} \quad (9)$$

Flowcell, integrated fluidic and imaging system

The flowcell, fluidic setup, and imaging system are essentially the same as described in our previous report (16). Briefly, the channels in the flowcell are formed between a coverslip and an anodized aluminum plate using double-sided silicone tape with 40 mm × 2 mm × 100 μm cutouts. The modular flow cell is mounted into a temperature control unit which consists of thermoelectric modules sandwiched between the block and a liquid-cooled aluminum heatsink mounted on a motorized XY microscope stage

(Bioprecision 2, Ludl Electronics Product). Fluid control is managed by a syringe pump connected to a nine-port rotary valve. The objective-based TIRF system consists of an inverted fluorescence microscope and a TIRF slider (AxioObserver Z1 and TIRF 3 Slider, Carl Zeiss). A 100× oil objective lens with a NA of 1.46 (Alpha Plan Apochromat, Carl Zeiss) is used for both laser excitation and fluorescence detection. The laser excitation is provided by a diode-pumped solid-state 532 nm laser. The excitation power is measured at the exit of the objective. The Cy3 emitted fluorescence is reflected by a dichroic mirror and passed through an emission filter (dichroic beamsplitter: Semrock Di01-R532-25×36; bandpass filter: Semrock FF01-560/25-25 with center at 560 nm and a bandwidth of 25 nm) and detected by an EMCCD camera (512 pixels × 512 pixels; 16 μm × 16 μm per pixel; iXon3 897, Andor Technology). Proper focus is maintained using an autofocus system. All components are controlled through a computer using custom software to automate the entire process, including temperature control, delivery of solutions, the initiation of the reactions, and fluorescence imaging.

Preparation of surfaces and fluidic devices for measuring incorporation kinetics

The DNA templates are covalently tethered to the surface of No. 1.5 glass coverslips through a series of chemical and biochemical processing steps. Aminosilane coated coverslips were transformed to a carboxylate surface by reacting the amine groups with dicarboxyl-PEG1000 at 2 mM in dry *N,N*-dimethylformamide (DMF) containing 20 mM 1-ethyl-3-(3-dimethylaminopropyl)carbodiimide hydrochloride (EDC) and 10 mM triethylamine (TEA) for 2 h at room temperature. After rinsing with methanol and DMF, the coverslips were soaked for 1 h in a DMF solution containing 250 mM succinic anhydride and 250 mM TEA to convert any remaining amine groups on the surfaces to carboxylate groups. The coverslips were rinsed three times with methanol and blown dry with argon. Finally, the 5' end of 50-base polydeoxythymidine (poly(dT)₅₀) oligonucleotides were covalently attached to the carboxylate groups on the surface using EDC chemistry by coating the coverslips in a solution containing 5 μM of 5'-amine-labeled poly(dT)₅₀ and 10 mM EDC in 100 mM (*N*-morpholino) ethanesulfonic acid buffer at pH 5.0 with 0.02% Triton X-100 for 2 h. After washing twice with 2× saline sodium citrate with 0.02% Triton-X100 (2× SSCt) and rinsing with deionized water, the functionalized coverslips were kept in 2× SSCt at 4°C until use.

After the functionalized coverslips were assembled into a flowcell, the template DNA was enzymatically synthesized on the surface of the channels by using the poly(dT)₅₀ on the surface as the primer to replicate a complementary sequence (5'-CCA GAG CCT CCA ACG CCA TAG TAC CAT CGC TTC GTT TCT TTT GTT TTT CAT CAG TCA TGT ACG AAG TCA GTC ATG CTA GTT TTA CCC CAC TAA GTC TGT A-3') to which a poly(dA) tail had been added. The poly(dA) tail was added by incubating 1 μM of the oligo in a solution containing 250 μM CoCl₂, 2 mM dATP, 50 mM potassium acetate, 20 mM Tris-acetate, 10 mM magnesium acetate, pH 7.9 and

0.67 units/ μl of terminal deoxyribonucleotidyl transferase at 37°C for 1 h, followed by thermal inactivation of the enzyme at 70°C for 10 min. Approximately 150 adenosine bases were added to the 3' end of the oligo under this condition. The polyadenylated oligo was hybridized to the poly(dT)₅₀ on the glass surface in the microfluidic channels by injecting 0.25 μM oligo in 2 \times SSCt and incubating the solution at room temperature for 15 min. After the channels were washed with a buffer solution of 100 mM NaCl, 10 mM Tris-HCl pH 8, 1 mM EDTA, and 0.02% Triton X-100 (T100 buffer), a reaction mix containing 100 $\mu\text{g/ml}$ BSA, 500 μM dNTPs, 20 mM Tris-HCl pH 8.8, 10 mM (NH₄)₂SO₄, 10 mM KCl, 2 mM MgSO₄, 0.1% Triton X-100 and 0.4 units/ μl Bst DNA polymerase large fragment was injected into the channels and incubated at 50°C for 10 min to synthesize the template DNA. The 3'-OH ends of the surface-bound oligos were capped with a dideoxyadenosine triphosphate (ddATP) by incubating a solution containing 1 mM ddATPs, 100 $\mu\text{g/ml}$ BSA, 50 mM NaCl, 10 mM Tris-HCl pH8, 10 mM MgCl₂ and 0.25 units/ μl Klenow Fragment (3'→ 5' exo-) DNA polymerase in the channels at 37°C for 15 min. The complementary sequence was then denatured and removed by flowing a buffered formamide solution (99% formamide, 10 mM Tris-HCl pH 8, 1 mM EDTA and 0.02% Triton X-100) preheated at 85°C through the channels. Finally, the channels were washed with T100 buffer and stored in the same buffer until use.

Real-time measurements of nucleotide incorporation kinetics

A set of Cy3-labeled dNTPs was used to enable single-turnover measurements using real-time TIRF microscopy. A specific primer was hybridized to the DNA template for the incorporation of each of the four bases. The sequences of the template and the four primers used are listed in Table 1. The hybridization was performed in each channel by injecting 1 μM of the primer in 2 \times SSCt at room temperature for at least 5 minutes. The channel was then washed briefly with T100 buffer. Duplicate measurements were carried out for each nucleotide using a reaction mix containing the specific nucleotide (Cy3-labeled, or a mixture of Cy3-labeled and native nucleotide at the specified ratio), 100 $\mu\text{g/ml}$ BSA, 5 mM PCA, 2 mM Trolox, 150 nM PCD, 50 mM NaCl, 10 mM Tris-HCl pH 8 and 10 mM MgCl₂, and 0.25 U/ μl (~185 nM) Klenow fragment of *E. coli* DNA polymerase I. PCA and PCD were included as oxygen scavenging system to reduce the oxidative damage and photobleaching of the fluorophores while Trolox was included to suppress blinking (17). Each single-turnover incorporation reaction was performed at 25°C by injecting the specific reaction mix into the channel at a linear flow rate of 100 mm/s and time-lapse TIRF images were immediately acquired using an exposure time from 50 to 100 ms and gain values from 50 to 100. The power of the 532 nm laser excitation measured at exit of the objective was between 0.2 and 4.0 mW. The excitation power, exposure times, and gain value were varied, depending on the concentration of fluorescent nucleotide in solution, to maximize dynamic range and sensitivity while minimizing photobleaching. The surface of the channel could be regenerated for multiple uses by denaturing and removing the extended products from

the DNA templates covalently attached to the surface. This was performed by flowing buffered formamide preheated at 85°C through the channels and a brief wash with T100 buffer. The dissociation constant and turnover number for each Cy3-labeled nucleotide were determined using pure labeled nucleotide with a series of concentrations from 0.5 to 16 μM . To determine the kinetic parameters of the native nucleotides, the kinetics of the competitive incorporation reactions were measured by using a mixture of labeled and the corresponding native nucleotide at a ratio of nine to one with total concentrations ranging from 0.25 to 16 μM .

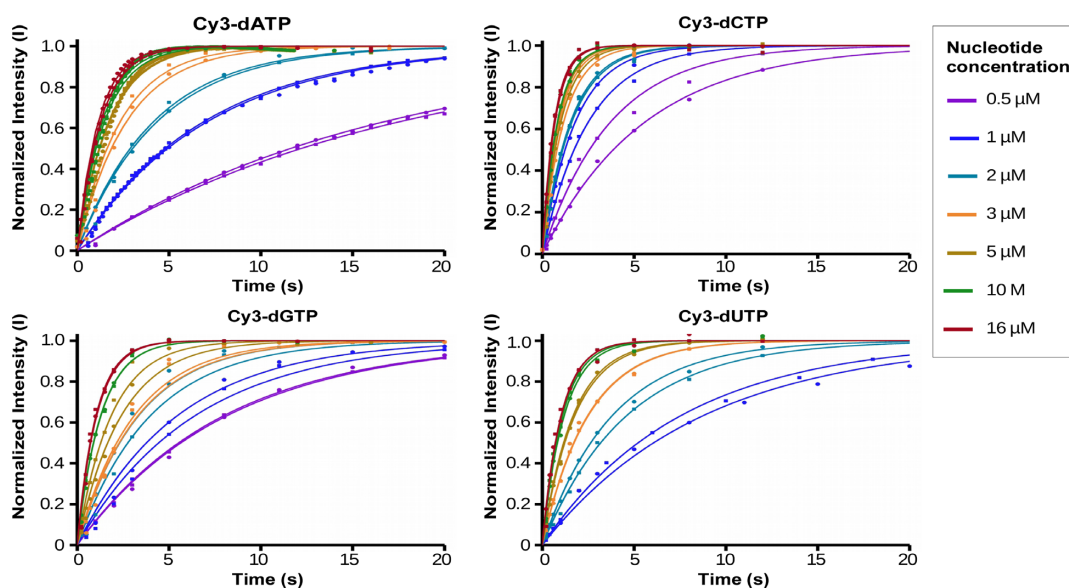
To appreciate the amount of effort required for the kinetics measurements, we estimate the time to acquire each kinetics trace and the entire dataset. The synthesis of covalently bound DNA templates was usually performed in all nine fluidic channels of the flow cell simultaneously in about 60 min. The prepared templates are stable for at least one week and each fluidic channel can be re-used for up to 10 incorporation reactions with minimal build-up of background and very little decrease in signal intensity. The hybridization of specific primers to the templates was performed within 2 min, and acquisition of the kinetics trace of each incorporation reaction required <1 min. The denaturation and removal of the extended primer to prepare the channel for the next kinetic measurement required 1 min. Therefore, once the templates have been prepared and the instrument has been set up, kinetics measurements could be performed at a rate of 5 min per kinetic trace. Our fully automated system with 9-channel flow cells allowed us to acquire the entire data set of 120 kinetics traces, which included duplicate measurements of each of the four pure labeled nucleotides at seven different concentrations and duplicate measurements of each of the four different nucleotides with a 9:1 labeled to native ratio at eight different concentrations. In theory, the entire data set could be acquired in <24 h with minimal hands-on time.

Image processing and data analysis

All image processing and data analysis was performed using MATLAB (MathWorks). The time-lapse images were processed by calculating the average fluorescence intensity value of all the pixels in each image. From Equation (8), the reaction is expected to be pseudo first-order. Therefore, fluorescence intensity values were plotted as a function of time and the curve was fit to a single exponential using the equation $I(t) = a(1 - e^{-bt}) + c$, where $I(t)$ is the intensity value at time t , a is a scaling factor for the total change in intensity increase, b is the observed reaction rate constant, and c represents the baseline intensity value. For visual comparisons between the data sets, the intensity values were normalized by subtracting each data point by the baseline intensity value c and dividing the value by the scaling factor a . Derivation of the equations was a little bit involved requiring some effort. Data analysis, however, was relatively straightforward using a readily available software package (MATLAB).

Table 1. Sequences of DNA template and primers used for nucleotide incorporation kinetic measurements. For clarity, only the priming region of the template sequence is shown

Oligonucleotide	Sequence
Template	3'-GGTCTCGGAGGTTGCGGTATCATGGTAGCGAAGCAA...-5'
Primer for incorporating dATP	5'-CCAGAGCCTCCAACGCCATAGTACC-3'
Primer for incorporating dTTP	5'-CCAGAGCCTCCAACGCCATAGTACCA-3'
Primer for incorporating dCTP	5'-CCAGAGCCTCCAACGCCATAGTACCAT-3'
Primer for incorporating dGTP	5'-CCAGAGCCTCCAACGCCATAGTACCATC-3'

**Figure 2.** Kinetics of incorporation of pure labeled nucleotides. Duplicate measurements were performed for each nucleotide concentration and the data and fits are represented with the same color. The number of data points for each trace varies depending on the kinetics. Each curve was fit to a single exponential, $I(t) = a(1 - e^{-bt}) + c$, where $I(t)$ is the intensity value at time t , a is a scaling factor for the total change in intensity increase, b is the observed reaction rate constant, and c is the baseline intensity value. The data shown has been normalized by subtracting the raw intensity values by c then dividing by a .

RESULTS

Measurements of nucleotide incorporation kinetics

To simplify our analysis, the reactions were performed with a very large excess of nucleotide concentration to the concentration of the DNA polymerase and template complex on the surface. The binding of DNA polymerase to DNA template is very rapid (18). Under our experimental conditions, the single-turnover nucleotide incorporation is expected to be a pseudo first-order reaction with respect to the polymerase template complex ($\text{Pol}\cdot\text{DNA}_n$). The measured fluorescence intensity from the surface is directly proportional to the single-base extension product with a labeled nucleoside incorporated ($[\text{Pol}\cdot\text{DNA}_{(n+1)\text{F}}]$). According to our kinetic model (Equation 8), the intensity trace as a function of reaction time is expected to be a single exponential. The catalytic rate constants and nucleotide binding dissociation constants of the labeled nucleotides were determined by measuring the kinetics of incorporation of the individual pure Cy3-labeled nucleotides at a series of nucleotide concentrations ranging from 0.5 to 16 μM . The normalized data and the fits for duplicate measurements are shown in Figure 2. Kinetic measurements of the competitive reactions between the incorporation of individual Cy3-labeled nucleotides and their corresponding native nucleotides were carried out using a 9:1 molar ratio of labeled

nucleotide to native nucleotide at a series of total nucleotide concentrations ranging from 0.25 to 16 μM . The large ratio was necessary to attain a sufficient level of incorporation of the labeled nucleotide to produce a good signal to noise in fluorescence imaging due to the significant bias of Klenow fragment of *E. coli* DNA polymerase I toward the native nucleotides against the labeled nucleotides. This ratio is unique depending on the bias toward the native nucleotides over the fluorescent nucleotides by the polymerase. As long as the polymerase can incorporate labeled nucleotides to some degree, our method can be applied. For polymerases with large bias, however, a high ratio of labeled to native nucleotides is necessary to achieve a sufficient level of labeled nucleotide incorporation to acquire measurements with good signal to noise. The normalized data and fits for duplicate measurements are displayed in Figure 3. All the curves in Figures 2 and 3 display the expected trend of faster incorporation rates at higher nucleotide concentrations and are fitted well to a single exponential, with an R^2 value >0.98 for most of the fits. The data from the duplicate measurements are very similar in most cases, indicating the consistency in the reaction kinetics and the experimental reproducibility of our method.

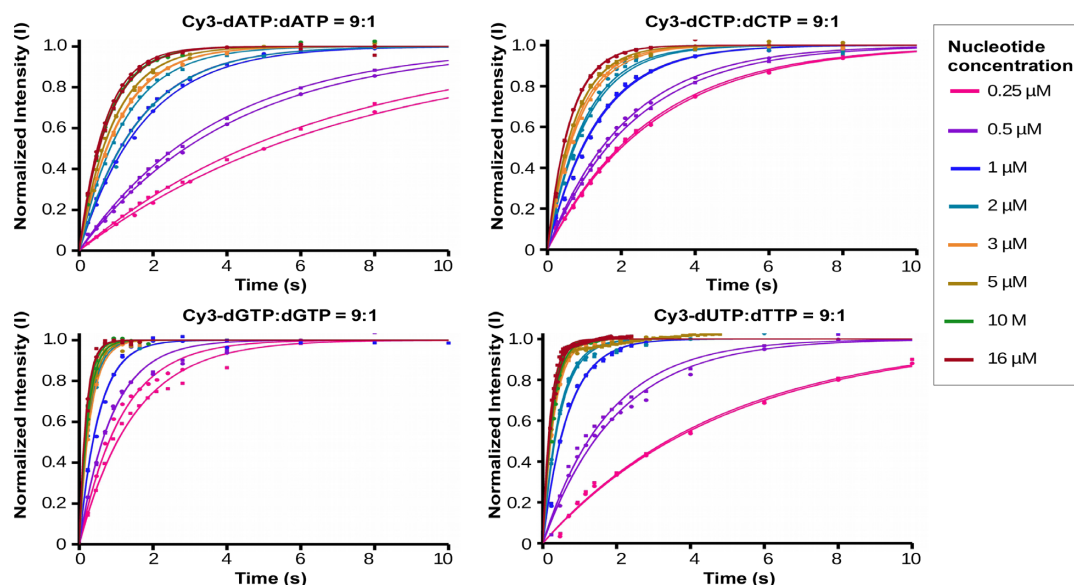


Figure 3. Kinetics of parallel competitive reactions in the incorporation of labeled nucleotide and native nucleotide. The ratio of the labeled nucleotide to the corresponding native nucleotide is kept constant at 9:1 while the total nucleotide concentration is varied from 0.25 to 16 μM . The measured fluorescence intensity is contributed only by the labeled nucleoside incorporated. As compared to the kinetics of pure labeled nucleotide, the observed kinetics is faster due to the competitive incorporation of the native nucleotide as expected. Each curve is fit to a single exponential as described in Figure 2. The data and fits for the duplicate measurements of each nucleotide concentration are represented with the same color.

Determination of rate constants and Michaelis constants

The observed rate constants were obtained from the kinetic data by fitting each curve to a single exponential as described earlier. The observed rate constants are then plotted as a function of nucleotide concentrations. The plots are shown in Figure 4. Based on our kinetics model, the curves are expected to be similar to the familiar Michaelis–Menten enzyme kinetics since the observed rate constant is the exponent in Equation (8) and is related to the total nucleotide concentration for a fixed ratio of labeled to native nucleotide concentration (r) by:

$$k_{\text{observed}} = \frac{(k_{2F}K_{MF}^{-1}r + k_{2N}K_{MN}^{-1})(K_{MF}^{-1}r + K_{MN}^{-1})^{-1}[\text{dNTP}_{\text{Total}}]}{(K_{MF}^{-1}r + K_{MN}^{-1})^{-1}(1+r) + [\text{dNTP}_{\text{Total}}]} \quad (10)$$

There are four kinetic parameters (k_{2F} , K_{MF} , k_{2N} , and K_{MN}) to be determined. They cannot be extracted directly by fitting the curves using Equation (10). Our strategy is to first determine the parameters for the labeled nucleotides (k_{2F} and K_{MF}) by measuring the incorporation kinetics of pure labeled nucleotides. In this case, $r = \infty$, Equation (10) is reduced to one with only two parameters (k_{2F} and K_{MF}):

$$k_{\text{observed}} = \frac{k_{2F}[\text{dNTP}_{\text{Total}}]}{K_{MF} + [\text{dNTP}_{\text{Total}}]} \quad (11)$$

The rate constants (k_{2F}) and Michaelis constants (K_{MF}) for the labeled nucleotides were obtained by fitting each curve using Equation (11) in a manner essentially the same as described in our previous report (16). As expected the curves are fitted well with R^2 values greater than 0.98. The fitted curves are shown in Figure 4A and the extracted k_2 and k_M values of the four Cy3-labeled nucleotides are listed in Table 2. Once these values are obtained, the curves from the competitive reactions between the labeled and native nu-

cleotides are the fitted using Equation (10) to extract the kinetics parameters (k_{2N} , and K_{MN}) of the native nucleotides. As expected, the curves are also fitted well with R^2 values >0.98 . The fitted curves are shown in Figure 4B and the extracted k_2 and k_M values of the native nucleotides are listed in Table 2. The error values reported in the table represent the 95% confidence bounds for the kinetic parameter fits.

DISCUSSION

We have demonstrated the ability to determine the kinetics of single-turnover incorporation of native nucleotides by DNA polymerase using time-lapse TIRF microscopy by measuring the parallel competitive incorporation reactions between native and fluorescently-labeled nucleotides on the surface of a microfluidic device. The nucleotide incorporation reactions were set up as pseudo first-order reactions with respect to the primed DNA template by using a large excess of nucleotides. By modeling the parallel competitive reactions and using a fixed ratio of labeled to native nucleotide concentration, the measured fluorescence intensity can be expressed as a function of five parameters, including the rate constants and Michaelis constants of both the native and labeled nucleotides, and the total nucleotide concentration (Equation 8). Two parameters, the catalytic rate constant and nucleotide binding dissociation constant of the labeled nucleotides are first determined using 100% labeled nucleotides. By measuring the kinetics of the competitive reactions between the native and labeled nucleotides using a fixed molar ratio of labeled nucleotide to native nucleotide at a series of total nucleotide concentrations, the single-turnover catalytic rate constants and the Michaelis constants of the native nucleotides can then be determined.

In our model, only the steady-state approximation to the intermediate complexes was made since intermediate

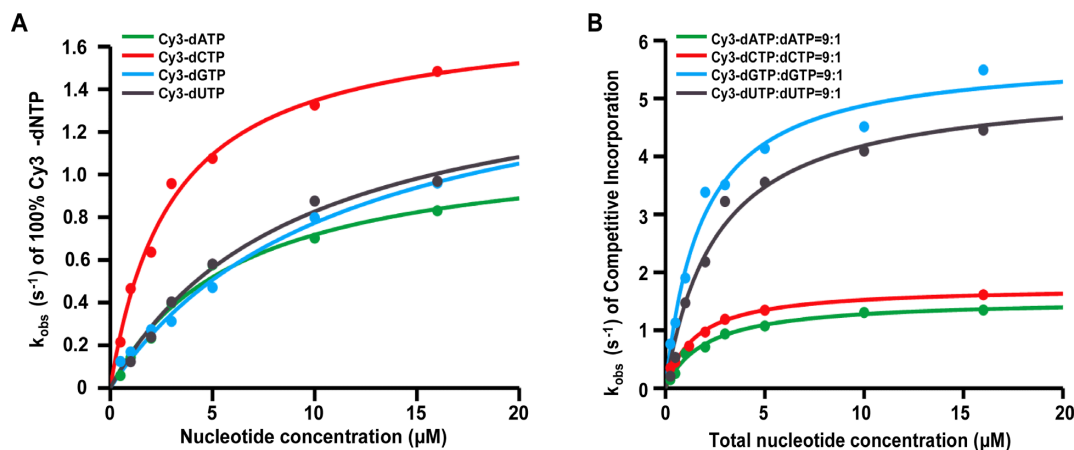


Figure 4. Observed reaction rate constants as a function of nucleotide concentrations. (A) The observed reaction rate constants for 100% labeled nucleotides over a range of concentrations. Each rate constant is the average value of the rate constants from duplicate measurements. The curves are fitted to extract the catalytic rate constants and Michaelis constants of the labeled nucleotides. (B) The observed rate constants of the competitive reactions at 9:1 molar ratio of labeled nucleotides to their corresponding native nucleotides. Each rate constant is the average value of the rate constants from duplicate measurements. The curves are fitted to extract the catalytic rate constants and Michaelis constants of the native nucleotides. The values are listed in Table 2.

Table 2. Incorporation kinetics of labeled and native nucleotides by Klenow fragment of *E. coli* DNA polymerase I. All measurements were performed in duplicate. The errors values are the bounds of the fitted values of the parameters at 95% confidence level

	Cy3-dATP	dATP	Cy3-dCTP	dCTP	Cy3-dGTP	dGTP	Cy3-dUTP	dTTP
k_2 (s^{-1})	1.16 ± 0.25	1.69 ± 0.26	1.75 ± 0.19	1.75 ± 0.29	1.64 ± 0.47	6.48 ± 1.09	1.57 ± 0.44	6.57 ± 1.74
K_M (μM)	6.23 ± 2.94	0.28 ± 0.12	3.00 ± 0.93	0.27 ± 0.14	11.2 ± 5.88	0.22 ± 0.10	8.93 ± 4.96	0.35 ± 0.11
k_2/K_M ($s^{-1} \cdot \mu M^{-1}$)	0.186 ± 0.097	6.04 ± 2.75	0.583 ± 0.192	6.48 ± 3.53	0.146 ± 0.088	29.5 ± 14.3	0.176 ± 0.110	18.8 ± 7.72

complexes usually do not accumulate to observable level in most enzyme catalysis, including DNA synthesis by DNA polymerases. Our data can be fitted very well using our model. This indicates that the steady-state approximation is very likely valid. The rates of nucleotide binding to the polymerase–primer/template complex and the dissociation of nucleotide from the complex are also known to be much faster than that of nucleotide incorporation ($k_{-1} \gg k_2$) (2), therefore, a rapid equilibrium is usually assumed to establish between the binding and dissociation of nucleotides. In this case, $K_M ((k_{-1} + k_2)/k_1)$ approximately equals to $K_d (k_{-1}/k_1)$, which quantifies the binding affinity of the nucleotide to the DNA polymerase.

To demonstrate our method, we used the well-characterized Klenow fragment of *E. coli* DNA polymerase I for this study. Steady-state and single-turnover incorporation kinetics of native nucleotides by this polymerase have been characterized using rapid quench-flow and other methods. It is worthwhile to look into whether the catalytic rate constants and dissociation constants obtained using our method are in line with those reported in the literature using other more conventional methods. Because of the relative paucity of data on single-turnover incorporation kinetics of labeled nucleotides by DNA polymerases, no extensive comparison can be made between the methods. Using rapid chemical-quench-flow method, Bower *et al.* determined the kinetics for the incorporation of dUTP labeled with a Cy5 dye via a disulfide linker by a mutant Klenow fragment without 3' to 5' exonuclease activity (Klenow exo-) (19) and reported a k_2 value of $2.4 s^{-1}$ and a K_M value of $4.9 \mu M$ (20). These values closely match the values we obtained for the incorporation of Cy3-dUTP by

the Klenow fragment. This is expected considering that the structures of the dyes and the linkers are very similar, and the polymerases are essentially identical since it has been shown that the mutations of two residues in the Klenow fragment to inactivate the 3' to 5' exonuclease activity do not affect the kinetics of polymerase reaction (21).

The catalytic rate constants (k_{cat} , or k_2 in our model) and dissociation constants or Michaelis constants (K_d or K_M) of incorporation of the some native nucleotides by Klenow fragment have been reported in the literature with a large range of values. Some of the early work based on the rapid chemical-quench method reported a k_{cat} value of $\sim 2.6 s^{-1}$ and K_M value of $0.2 \mu M$ for the incorporation of dTTP by *E. coli* DNA polymerase I at $22^\circ C$ (22). Measurements made by Niikura *et al.* using a different method, in which the incorporation kinetics was directly monitored with a quartz microbalance, gave similar values (23). These values are also in the ranges of the steady-state kinetics reported for the incorporation of dTTP into long poly(dA) templates ($k_{cat} = 2.8 s^{-1}$ and $K_M = 2.3 \mu M$) (21) and dGTP ($k_{cat} = 1.2 s^{-1}$ and $K_M = 0.4 \mu M$) at $22^\circ C$ (24). Overall, the k_{cat} and K_M values for the incorporation of native nucleotides by Klenow fragment determined using our method (Table 2) are roughly in the ranges of those reported values. The kinetics of nucleotide incorporation by DNA polymerase is known to be sequence context dependent and can be influenced by reaction conditions such as pH, concentration of Mg^{2+} and temperature. Therefore, the single-turnover kinetics is expected to vary to some degree depending on the sequence of the DNA template.

To evaluate the soundness and limitations of our method, we consider several factors related to polymerase properties,

reaction conditions and technical capability of our instrument. First, the Klenow fragment retains the 3'→5' exonuclease activity of the polymerase I, which could potentially affect the kinetics of the measurements. However, the rate constant of the exonuclease activity for double-stranded DNA is reported to be on the order of 10^{-3} s^{-1} , which is several orders of magnitude slower than that of nucleotide incorporation (25). Therefore, its exonuclease activity is not considered to have a measurable effect on our kinetic measurements. Incubation of Klenow fragment in the absence of nucleotides in the fluidic channel after an incorporation reaction has been performed resulted in a negligible decrease in fluorescent signal over 20 s, the duration over which the incorporation reactions were monitored (data not shown). This indicates that exonucleolysis does not have an effect on the incorporation kinetic measurements. Second, due to the presence of the 3'→5' exonuclease activity of the Klenow fragment, the polymerase is not pre-bound onto the primer-DNA template on the surface. Instead, a very high concentration of the polymerase (~185 nM in final reaction mix) is added into the nucleotide reaction solution and the reaction is initiated by injecting the solution into the microfluidic channels. The kinetics of polymerase binding to the DNA templates on the surface could also affect the measurements of the nucleotide incorporation kinetics. However, the kinetics of binding of polymerases to primer-DNA templates is known to be very rapid at high concentrations of polymerases. If the binding of Klenow fragment to the surface-bound template was occurring on a similar time scale as the reaction kinetics of nucleotide incorporation, the kinetics trace would not follow a single exponential fit which is characteristic of a first-order reaction. Therefore, the kinetics of binding of polymerase to the DNA templates on the surface is expected to have no or very little effect on our kinetics measurements. Third, very fast kinetics measurements could be limited by the speed of initiation of the reaction and detection. As described in more detail in our previous report (16), a reaction mix can be delivered into the detection window of the EMCCD camera in <1 ms using our microfluidic device, and up to 1 ms per frame (1000 frames per second) can easily be achieved with EMCCD and sCMOS cameras with or without binning.

In this work, we presented, for the first time, the systematic measurements of the single-turnover kinetics, including the apparent catalytic rate constants and Michaelis constants, of a complete set of all four labeled and native nucleotides. From the measured kinetics parameters, several interesting observations can be made. First, the attachment of the Cy3 label to the nucleobases has very little effect on the rates of incorporation of Cy3-dATP and Cy3-dCTP while the modification has a significant effect on the incorporation rate of Cy3-dGTP and Cy3-dUTP, reducing the rate by ~4-fold. Second, the attachment of the label to the nucleobases significantly reduces the K_M or the binding affinity of polymerase to the labeled nucleotides, by as much as 10 to 50 fold when compared to K_M or affinity of the polymerase to their corresponding native nucleotides. Overall, the chemical modification on the nucleobases results in a large polymerase bias toward the native nucleotides over the Cy3-labeled nucleotides, by as much as 200 fold if the bias is quantified using the

k_{cat}/k_M criterion. The ratios of the k_{cat}/k_M values are 32:1, 11:1, 201:1 and 107:1 for dATP/Cy3-dATP, dCTP/Cy3-dCTP, dGTP/Cy3-dGTP and dTTP/Cy3-dUTP, respectively. Third, the chemical modification has a different effect on different nucleotides. The combined effect of rate and affinity results in a significant bias against some labeled nucleotides such as Cy3-dGTP.

Our reported method provides an alternative to the commonly used stopped-flow or rapid quench-flow method for the direct and fully automated measurements of kinetics of nucleotide incorporation by DNA polymerases, and perhaps other enzymatic reactions as long as there is a means to capture the fluorescent substrates or the reaction products on the surface. By setting up parallel competitive reactions between a native nucleotide and the corresponding labeled nucleotide, our strategy allows for the incorporation kinetics of native and other non-fluorescent nucleotides to be directly monitored in a rapid and automated fashion. At present, nucleotide incorporation kinetics data are available for a relatively small set of the DNA and RNA polymerases that are commonly employed in genomic and molecular biology applications. A facile and fully automated method as we reported here will enable the acquisition of the kinetics data for mechanistic studies of DNA polymerases and other enzymes, and practical applications such as the development and improvement of DNA sequencing technologies. In fact, our method was developed to enable a novel sequencing strategy called natural sequencing by synthesis (nSBS), in which a small percent of non-terminating fluorescently labeled nucleotides is incorporated along with the corresponding native base (26).

SUPPLEMENTARY DATA

Supplementary Data are available at NAR Online.

FUNDING

National Institutes of Health [HG007836]. Funding for open access charge: National Institutes of Health.

Conflict of interest statement. None declared.

REFERENCES

1. Kunkel, T.A. (2009) Evolving views of DNA replication (in)fidelity. *Cold Spring Harb. Symp. Quant. Biol.*, **74**, 91–101.
2. Johnson, K.A. (2010) The kinetic and chemical mechanism of high-fidelity DNA polymerases. *Biochim. Biophys. Acta*, **1804**, 1041–1048.
3. Xia, S. and Konigsberg, W.H. (2014) RB69 DNA polymerase structure, kinetics, and fidelity. *Biochemistry*, **53**, 2752–2767.
4. Joyce, C.M. and Benkovic, S.J. (2004) DNA polymerase fidelity: kinetics, structure, and checkpoints. *Biochemistry*, **43**, 14317–14324.
5. Giller, G., Tasara, T., Angerer, B., Muhlegger, K., Amacker, M. and Winter, H. (2003) Incorporation of reporter molecule-labeled nucleotides by DNA polymerases. I. Chemical synthesis of various reporter group-labeled 2'-deoxyribonucleoside-5'-triphosphates. *Nucleic Acids Res.*, **31**, 2630–2635.
6. Schena, M., Shalon, D., Davis, R.W. and Brown, P.O. (1995) Quantitative monitoring of gene expression patterns with a complementary DNA microarray. *Science*, **270**, 467–470.
7. Randolph, J.B. and Waggoner, A.S. (1997) Stability, specificity and fluorescence brightness of multiply-labeled fluorescent DNA probes. *Nucleic Acids Res.*, **25**, 2923–2929.

8. Ju, J., Kim, D.H., Bi, L., Meng, Q., Bai, X., Li, Z., Li, X., Marma, M.S., Shi, S., Wu, J. *et al.* (2006) Four-color DNA sequencing by synthesis using cleavable fluorescent nucleotide reversible terminators. *Proc. Natl. Acad. Sci. U.S.A.*, **103**, 19635–19640.
9. Eid, J., Fehr, A., Gray, J., Luong, K., Lyle, J., Otto, G., Peluso, P., Rank, D., Baybayan, P., Bettman, B. *et al.* (2009) Real-time DNA sequencing from single polymerase molecules. *Science*, **323**, 133–138.
10. Bentley, D.R., Balasubramanian, S., Swerdlow, H.P., Smith, G.P., Milton, J., Brown, C.G., Hall, K.P., Evers, D.J., Barnes, C.L., Bignell, H.R. *et al.* (2008) Accurate whole human genome sequencing using reversible terminator chemistry. *Nature*, **456**, 53–59.
11. Metzker, M.L., Raghavachari, R., Burgess, K. and Gibbs, R.A. (1998) Elimination of residual natural nucleotides from 3'-O-modified-dNTP syntheses by enzymatic mop-up. *Biotechniques*, **25**, 814–817.
12. Frey, M.W., Sowers, L.C., Millar, D.P. and Benkovic, S.J. (1995) The nucleotide analog 2-aminopurine as a spectroscopic probe of nucleotide incorporation by the Klenow fragment of Escherichia-coli polymerase-I and bacteriophage-T4 DNA-polymerase. *Biochemistry*, **34**, 9185–9192.
13. Gong, P., Campagnola, G. and Peersen, O.B. (2009) A quantitative stopped-flow fluorescence assay for measuring polymerase elongation rates. *Anal. Biochem.*, **391**, 45–55.
14. Tsai, Y.C., Jin, Z. and Johnson, K.A. (2009) Site-specific labeling of T7 DNA polymerase with a conformationally sensitive fluorophore and its use in detecting single-nucleotide polymorphisms. *Anal. Biochem.*, **384**, 136–144.
15. Tsai, Y.C. and Johnson, K.A. (2006) A new paradigm for DNA polymerase specificity. *Biochemistry*, **45**, 9675–9687.
16. Walsh, M.T., Roller, E.E., Ko, K.S. and Huang, X. (2015) Measurement of DNA polymerase incorporation kinetics of dye-labeled nucleotides using total internal reflection fluorescence microscopy. *Biochemistry*, **54**, 4019–4021.
17. Aitken, C.E., Marshall, R.A. and Puglisi, J.D. (2008) An oxygen scavenging system for improvement of dye stability in single-molecule fluorescence experiments. *Biophys. J.*, **94**, 1826–1835.
18. Markiewicz, R.P., Vrtis, K.B., Rueda, D. and Romano, L.J. (2012) Single-molecule microscopy reveals new insights into nucleotide selection by DNA polymerase I. *Nucleic Acids Res.*, **40**, 7975–7984.
19. Derbyshire, V., Freemont, P.S., Sanderson, M.R., Beese, L., Friedman, J.M., Joyce, C.M. and Steitz, T.A. (1988) Genetic and crystallographic studies of the 3', 5'-exonucleolytic site of DNA polymerase I. *Science*, **240**, 199–201.
20. Bowers, J., Mitchell, J., Beer, E., Buzby, P.R., Causey, M., Efcavitch, J.W., Jarosz, M., Krzymanska-Olejnik, E., Kung, L., Lipson, D. *et al.* (2009) Virtual terminator nucleotides for next-generation DNA sequencing. *Nat. Methods*, **6**, 593–595.
21. Polesky, A.H., Steitz, T.A., Grindley, N.D. and Joyce, C.M. (1990) Identification of residues critical for the polymerase activity of the Klenow fragment of DNA polymerase I from Escherichia coli. *J. Biol. Chem.*, **265**, 14579–14591.
22. Bryant, F.R., Johnson, K.A. and Benkovic, S.J. (1983) Elementary steps in the DNA polymerase I reaction pathway. *Biochemistry*, **22**, 3537–3546.
23. Matsuno, H., Niikura, K. and Okahata, Y. (2001) Direct monitoring kinetic studies of DNA polymerase reactions on a DNA-immobilized quartz-crystal microbalance. *Chemistry*, **7**, 3305–3312.
24. Astatke, M., Grindley, N.D. and Joyce, C.M. (1995) Deoxynucleoside triphosphate and pyrophosphate binding sites in the catalytically competent ternary complex for the polymerase reaction catalyzed by DNA polymerase I (Klenow fragment). *J. Biol. Chem.*, **270**, 1945–1954.
25. Kuchta, R.D., Benkovic, P. and Benkovic, S.J. (1988) Kinetic mechanism whereby DNA polymerase I (Klenow) replicates DNA with high fidelity. *Biochemistry*, **27**, 6716–6725.
26. Huang, X. and Roller, E.E. (2014) Mostly natural DNA sequencing by synthesis. Patent No. US 8772473 B2.